

# Inverse Delayed Reinforcement Learning

**Simon Sinong Zhan**<sup>\*1</sup>

**Qingyuan Wu**<sup>\*2</sup>

**Zhian Ruan**<sup>1</sup>

**Frank Yang**<sup>1</sup>

**Philip Wang**<sup>1</sup>

**Yixuan Wang**<sup>1</sup>

**Ruochen Jiao**<sup>1</sup>

**Chao Huang**<sup>2</sup>

**Qi Zhu**<sup>1</sup>

SINONGZHAN2028@U.NORTHWESTERN.EDU

QINGYUAN.WU@SOTON.AC.UK

ZHIANRUAN2025@U.NORTHWESTERN.EDU

FRANKYANG2024@U.NORTHWESTERN.EDU

PHILIPWANG2025@U.NORTHWESTERN.EDU

YIXUANWANG2024@U.NORTHWESTERN.EDU

RUOCHENJIAO2024@U.NORTHWESTERN.EDU

CHAO.HUANG@SOTON.AC.UK

QZHU@NORTHWESTERN.EDU

<sup>1</sup> *Department of Electrical and Computer Engineering, Northwestern University, USA*

<sup>2</sup> *School of Electronics and Computer Science, University of Southampton, UK*

## Abstract

Inverse Reinforcement Learning (IRL) has demonstrated effectiveness in a variety of imitation tasks. In this paper, we introduce an IRL framework designed to extract rewarding features from expert trajectories affected by delayed disturbances. Instead of relying on direct observations, our approach employs an efficient off-policy adversarial training framework to derive expert features and recover optimal policies from augmented delayed observations. Empirical evaluations in the MuJoCo environment under diverse delay settings validate the effectiveness of our method. Furthermore, we provide a theoretical analysis showing that recovering expert policies from augmented delayed observations outperforms using direct delayed observations.

**Keywords:** Imitation Learning; Inverse Reinforcement Learning; Delay in Cyber-Physical Systems

## 1. Introduction

Reinforcement Learning (RL) has achieved remarkable success across diverse domains, including video and board games (Berner et al., 2019; Silver et al., 2017), robotics (Kormushev et al., 2013), and safety-critical autonomous systems (Wang et al., 2023a,b; Zhan et al., 2024b). Despite these advancements, RL heavily relies on the quality of the reward function, which often demands significant domain expertise, labor, and time to design (Russell, 1998). To address this challenge, Kalman (1964) introduced the concept of the inverse problem of optimal control theory, providing a way to bypass explicit reward or cost function specification. With the integration of machine learning techniques, Imitation Learning (IL) has evolved into two main branches. Behavior Cloning (BC (Torabi et al., 2018)) directly learns from expert demonstrations by aligning with the distribution of expert behaviors. In contrast, Inverse Reinforcement Learning (IRL (Arora and Doshi, 2021)) focuses on extracting reward functions from expert behavior to guide policy learning. These methods have shown significant promise in real-world applications, including autonomous driving (Codevilla et al., 2018) and legged locomotion (Peng et al., 2020). However, expanding IL to broader applications still requires attention to address real-world environmental challenges, such as hybrid dynamic (Hempel

\*. These authors contributed equally to this work

et al., 2014; Su et al., 2024), stochasticity (Zhan et al., 2024a), and delays (Xue et al., 2020). In this paper, we consider IRL under the delay setting. Specifically, how can we extract rewarding features from expert trajectories when the provided trajectories are interfered with delays?

Delay disturbance is prevalent in nowadays timing-sensitive Cyber-Physical Systems applications (Xue et al., 2017; Feng et al., 2019; Liu et al., 2023) including robotics (Hwangbo et al., 2017; Mahmood et al., 2018), transportation systems (Cao et al., 2020), and financial trading (Hasbrouck and Saar, 2013), where feedback delays are inherent in actuation, transmission, and sensors processing (Sun et al., 2021, 2022). Under the RL formulation, delays can be primarily categorized into three sections, namely observation delay, action delay, and reward delay (Liotet et al., 2022). Unlike well-explored reward delay (Han et al., 2022; Zhang et al., 2023), observation delay and action delay disrupt the Markovian property of system dynamic, posing significant challenges to both RL and IRL methods. There are several methods to tackle the delayed RL problem. Augmentation-based approaches (Altman and Nain, 1992; Katsikopoulos and Engelbrecht, 2003b) reformulate the delayed RL problem back to the MDP by stacking the latest observed state with a sequence of actions that happened within the delay period transforming them into a new observation information state. Imitation-based approaches (Liotet et al., 2022; Xie et al., 2023; Wu et al., 2024b) formulate delayed RL into an imitation problem to the delay-free scenario through constructing explicit delay belief functions.

Despite the advancements in delayed RL, limited attention has been given to addressing delay in IRL. While some studies explore reward delays within the context of imitation learning (Krishnan et al., 2016, 2019), few—if any—consider observation or action delays, where the expert trajectories consist solely of delayed observations and corresponding action sequences. Addressing delay in IRL has significant implications across various applications. For instance, in teleoperated robotics, such as remote robotic surgery or underwater exploration, automating these tasks using imitation learning requires adapting to signal delays not only during deployment but also within the expert demonstrations themselves. The difficulties are the following: The temporal misalignment between the perceived state and corresponding actions renders direct behavior cloning infeasible. Moreover, this misalignment, coupled with the non-Markovian nature of delayed observations, exacerbates the inherent ill-posedness of IRL. This ill-posedness arises from the fact that multiple reward functions can potentially explain the expert behavior observed in the trajectories. Thus, the reward functions extracted from the delayed observation state might not be optimal for recovering the expert performance.

In this paper, we propose an off-policy framework for Inverse Delayed Reinforcement Learning (IDRL). By applying a state augmentation technique to both offline expert trajectories and online environmental interactions, our approach constructs a richer feature space that incorporates augmented state and action information. Using this augmented representation, we extract reward features that better capture the underlying dynamics. These reward signals are then integrated with state-of-the-art policy optimization methods, enabling our framework to achieve superior performance in recovering expert behavior compared to naive IRL baselines built on delayed observation states. Furthermore, we provide a theoretical analysis that justifies the use of augmented state representations over delayed observation states in the context of IRL, offering deeper insights into their effectiveness.

We first introduce related literature on Delayed RL and IRL in Section 2, following a brief background introduction for problem formulation (Section 3). In Section 4, we present a comprehensive theoretical analysis of the performance difference using different reward shaping. Inspired by the theoretical results, in Section 5, we specifically propose IDRL, an off-policy Inverse Delayed RL

method. In Section 6, we show that our IDRL significantly outperforms various baselines over different MuJoCo benchmarks.

## 2. Related Works

**Delayed RL.** Delayed signals within the RL setting can be categorized into three scenarios namely rewards delay, actions delay, and observations delay. Rewards delay has been studied extensively (Han et al., 2022; Arjona-Medina et al., 2019; Zhang et al., 2023), and in this study, we concentrate on observations and actions delay, which have also been proved to be the equivalent problem (Katsikopoulos and Engelbrecht, 2003b). Early approaches apply RL techniques to the original state space. While it maintains high computational efficiency, the performance significantly deteriorates in delayed observation due to the absence of Markovian property. Subsequent improvements leveraged various predictive models like deterministic generators (Walsh et al., 2009), Gaussian models (Chen et al., 2021), and transformer architectures (Liotet et al., 2021). Additionally, there are also attempts building upon the world model with delay adaption (Karamzade et al., 2024; Valensi et al., 2024). However, learning from the original state space cannot effectively compute approximation errors accumulated from observation delays, causing the performance to deteriorate with suboptimal solutions in delayed settings (Liotet et al., 2021). The augmentation-based approach augments the state/action space with relevant past actions/states. This approach is notably more promising as it restores the Markovian property (Altman and Nain, 1992; Katsikopoulos and Engelbrecht, 2003a; Kim et al., 2023; Wu et al., 2024a) but possesses inherent sample complexity/efficiency issues. Solving this issue, Wu et al. (2024b) proposes a novel framework to transfer the original delayed RL objective into a behavior cloning of the delay-free policy through variational inference techniques. In contrast to the number of delayed RL research, there are limited works in the delayed IRL setting.

**Inverse RL.** Early research in Inverse Optimal Control (IOC) (Kalman, 1964) focused on recovering optimal control rule that maximizes margins between expert demonstrations and alternative policies, which evolves into machine-learning version Inverse Reinforcement Learning (IRL)(Ng et al., 2000). Bayesian methodologies later explored varied reward priors - from Boltzmann distributions (Ramachandran and Amir, 2007; Choi and Kim, 2011; Chan and van der Schaar, 2021) to Gaussian Processes (Levine et al., 2011). Concurrent development on statistical approaches expanded the field through multi-class classification (Klein et al., 2012; Brown et al., 2019) and decision tree methods (Levine et al., 2010). Entropy-based optimization leverages the Maximum Entropy(ME) principle (Shore and Johnson, 1980) to determine trajectory distributions from reward parameters. Ziebart et al. (2008, 2010) reformulated reward inference as a maximum likelihood problem using a linear combination of hand-crafted features. Wulfmeier et al. (2015) extended it to deep neural network representation, while Finn et al. (2016) added importance sampling for model-free estimation. Inspired by Generative Adversarial Networks, the latest advances in IRL center on adversarial methods, where discriminator networks learn reward functions by distinguishing between expert and agent behaviors (Ho and Ermon, 2016; Fu et al., 2017). There are extensions to solve sample efficiency (Kostrikov et al., 2018; Blondé and Kalousis, 2019) and to solve stochasticity MDP issue (Zhan et al., 2024a). As for IRL under delayed scenarios, there has been some attention on delayed rewards (Krishnan et al., 2016, 2019). However, to our knowledge, few have considered delayed action and observations under IRL settings.

### 3. Preliminaries

In delay-free IRL setting, we consider a standard MDP without reward function  $\mathcal{M}'$  defined as a tuple  $\langle \mathcal{S}, \mathcal{A}, \mathcal{T}, \gamma, \rho \rangle$ , where  $\mathcal{S}$  is the state space  $s \in \mathcal{S}$ ,  $\mathcal{A}$  is the action space  $a \in \mathcal{A}$ ,  $\mathcal{T} : \mathcal{S} \times \mathcal{A} \times \mathcal{S} \rightarrow [0, 1]$  is the transition probability function,  $\gamma \in (0, 1)$  is the discount factor, and  $\rho_0$  is the initial state distribution. The discounted visitation distribution of trajectory  $\tau$  with policy  $\pi$  is given by:

$$p(\tau) = \rho_0 \prod_{t=0}^{T-1} \gamma^t \mathcal{T}(s_{t+1}|s_t, a_t) \pi(a_t|s_t), \quad (1)$$

where  $T$  is the horizon. Given an MDP  $\mathcal{M}'$  without reward and expert trajectories collected in a data buffer  $D_{exp} = \{\tau_1, \dots, \tau_n\}$  where  $\tau_i$  represents individual trajectories collected using expert demonstration policy  $\pi^E : \mathcal{S} \rightarrow \mathcal{A}$ , IRL infers reward function  $R_\theta : \mathcal{S} \times \mathcal{A} \rightarrow \mathbb{R}$ , where  $\theta$  is the reward parameter. Maximizing the entropy of distribution over paths subject to the feature constraints from observation (Ziebart et al., 2008, 2010), the optimal reward parameters are obtained by

$$\theta^* = \arg \max_{\theta} \sum_{D_{exp}} \log p(\tau|\theta). \quad (2)$$

Under delayed RL settings, we consider MDPs with an observation delay between the action taken and when its state transition and reward are observed, termed delayed MDPs. Assuming under a constant observation delay  $\Delta$ , a delayed MDP  $\mathcal{M}_\Delta$  inherits the Markov property based on the augmentation approaches (Altman and Nain, 1992; Katsikopoulos and Engelbrecht, 2003a). It can be formulated as a tuple  $\langle \mathcal{X}, \mathcal{A}, \mathcal{T}_\Delta, R_\Delta, \gamma, \rho_\Delta \rangle$ . The augmented state space is defined as  $\mathcal{X} := \mathcal{S} \times \mathcal{A}^\Delta$ , where an augmented state  $x_t = \{s_{t-\Delta}, a_{t-\Delta}, \dots, a_{t-1}\} \in \mathcal{X}$ . The delayed transition function is defined as:

$$\mathcal{T}_\Delta(x_{t+1}|x_t, a_t) := \mathcal{T}(s_{t-\Delta+1}|s_{t-\Delta}, a_{t-\Delta}) \delta_{a_t}(a'_t) \prod_{i=1}^{\Delta-1} \delta_{a_{t-i}}(a'_{t-i}), \quad (3)$$

where  $\delta$  is the Dirac distribution. The delayed reward function is defined as  $R_\Delta(x_t, a_t) := \mathbb{E}_{s_t \sim b(\cdot|x_t)} [R(s_t, a_t)]$  where  $b$  is the belief function defined as:

$$b(s_t|x_t) := \int_{\mathcal{S}^\Delta} \prod_{i=0}^{\Delta-1} \mathcal{T}(s_{t-\Delta+i+1}|s_{t-\Delta+i}, a_{t-\Delta+i}) ds_{t-\Delta+i+1}. \quad (4)$$

And the initial augmented state distribution is defined as  $\rho_\Delta = \rho_0 \prod_{i=1}^{\Delta} \delta_{a_{-i}}$ . Correspondingly, we can define the trajectory visitation probability in the delayed MDP  $\mathcal{M}_\Delta$  with policy  $\pi_\Delta$  as:

$$p(\tau_\Delta) = \rho_\Delta \prod_{t=0}^{T-1} \gamma^t \mathcal{T}_\Delta(x_{t+1}|x_t, a_t) \pi_\Delta(a_t|x_t). \quad (5)$$

Under the delayed IRL setting, expert trajectories exhibit temporal misalignment, where the observed sequence follows the pattern  $(s_{t-\Delta}, a_t, s_{t-\Delta+1}, \dots)$ . This misalignment raises a fundamental question: **what kind of representation should be used in reward shaping to recover the expert policy?** Specifically, the policy and reward can be conditioned on the delayed observation state  $s_{t-\Delta}$ ,

which directly corresponds to the provided trajectories, or on an augmented state representation  $x_t$  that accounts for the delay and incorporates additional context. The design of state representation is critical, as it directly affects the accuracy and robustness of the recovered policy. In the next section, we provide a theoretical analysis to address this question, offering insights into the trade-offs and advantages of each approach.

#### 4. Theoretical Analysis

In this section, we analyze the difference in optimal performance when the same IRL algorithm is applied using either the delayed observation state or the augmented state. It is important to note that the reward functions in these two cases are also defined differently depending on different inputs. To quantify this performance difference, we first examine the discrepancy between the recovered reward functions under each state representation. We then extend this analysis to evaluate the impact on the value function, assuming the same policy optimization method is used. We assume that learned reward functions and transition dynamic functions satisfy the Lipschitz Continuity (LC) property, which is a common assumption that appears in RL setting (Rachelson and Lagoudakis, 2010). And reward functions are bounded by a maximum value  $R_{\max}$ .

**Definition 1 (Lipschitz Continuous Reward Function (Rachelson and Lagoudakis, 2010))** *A reward function  $R$  is  $L_{\mathcal{R}}$ -Lipschitz Continuous, if,  $\forall (s_1, a_1), (s_2, a_2) \in \mathcal{S} \times \mathcal{A}$ , it satisfies*

$$d_{\mathcal{R}}(R(s_1, a_1) - R(s_2, a_2)) \leq L_{\mathcal{R}}(d_{\mathcal{S}}(s_1, s_2) + d_{\mathcal{A}}(a_1, a_2)).$$

**Definition 2 (Time Lipschitz Continuous Dynamic (Metelli et al., 2020))** *A dynamic is  $L_{\mathcal{T}}$ -Time Lipschitz Continuous, if,  $\forall (s_1, a_1), (s_2, a_2) \in \mathcal{S} \times \mathcal{A}$ , it satisfies*

$$W_1(\mathcal{T}(\cdot|s, a)||\delta_s) \leq L_{\mathcal{T}}.$$

where *Euclidean distance*  $d$  is adopted to describe distance in a deterministic space (e.g.,  $d_{\mathcal{S}}$  for state space  $\mathcal{S}$ ,  $d_{\mathcal{A}}$  for action space  $\mathcal{A}$  and  $d_{\mathcal{R}}$  for reward space  $\mathcal{R}$ ), and *L1-Wasserstein distance* (Villani et al., 2009), denoted as  $W_1$ , is used in a probabilistic space. From the above assumptions, we can infer the Lipschitz continuity on belief function. Detailed proof can be found in Appendix A.

**Lemma 3 (Time Lipschitz Continuous Belief)** *Given a  $L_{\mathcal{R}}$ -Time Lipschitz Continuous Dynamic, the belief  $b$  is  $L_{\mathcal{R}}$ -Time Lipschitz Continuous,  $\forall x_t \in \mathcal{X}$ , satisfying*

$$W_1(b(\cdot|x_t)||\delta_{s_{t-\Delta}}) \leq \Delta L_{\mathcal{R}}.$$

Next, we extend the continuity bounds to the learned reward functions defining on delayed observation state and augmented state respectively. Note that we assume both reward functions are recovered using the same IRL algorithm and are parameterized by MLP with ReLU activation, which satisfies the Lipschitz continuous assumption (Virmaux and Scaman, 2018). Details of the IRL algorithm and implementation are presented in Section 5, and the detailed proof is in Appendix A.

**Lemma 4 (Reward Delayed Difference Upper Bound)** *Given a  $L_{\mathcal{R}}$ -Time Lipschitz Continuous Dynamic and  $L_{\mathcal{R}}$ -Lipschitz Continuous Reward function,  $\forall x_t \in \mathcal{X}$ , the upper bound of reward delayed difference is as follows:*

$$d_{\mathcal{R}}(R_{\Delta}(x_t, a_t) - R(s_{t-\Delta}, a_t)) \leq \Delta L_{\mathcal{R}} L_{\mathcal{T}}.$$

With the difference bound on the reward function, we seek to extend this bound to value functions corresponding to different policies  $\pi$  and  $\pi_\Delta$ , which directly reflect the performance difference. We define the value function of  $\pi_\Delta$  as follows:

$$V^{\pi_\Delta}(x_t) = \mathbb{E}_{\substack{x_{t+1} \sim \mathcal{T}_\Delta(\cdot|x_t, a_t) \\ a_t \sim \pi_\Delta(\cdot|x_t)}} [R_\Delta(x_t, a_t) + \gamma V^{\pi_\Delta}(x_{t+1})]. \quad (6)$$

And the definition of the value function corresponding with  $\pi$  is the following.

$$V^\pi(x_t) = \mathbb{E}_{\substack{x_{t+1} \sim \mathcal{T}_\Delta(\cdot|x_t, a_t) \\ a_t \sim \pi(\cdot|x_{t-\Delta})}} [R(s_{t-\Delta}, a_t) + \gamma V^\pi(x_{t+1})]. \quad (7)$$

**Proposition 5 (Performance Difference Upper Bound)** *Given a  $L_{\mathcal{R}}$ -Time Lipschitz Continuous Dynamic,  $L_{\mathcal{R}}$ -Lipschitz Continuous Reward function, and policies  $\pi$  and  $\pi_\Delta$ ,  $\forall x_t \in \mathcal{X}$ , the upper bound of performance difference is as follows:*

$$\|V^{\pi_\Delta}(x_t) - V^\pi(x_t)\| \leq \frac{1}{1-\gamma} [R_{\max} + \Delta L_{\mathcal{R}} L_{\mathcal{T}}].$$

Detailed proof can be found in Appendix A. From Prop. 5, we provide a theoretical insight to choose augmented state  $x$  instead of delayed observation state to recover value function.

## 5. Off-Policy Inverse Delayed RL

In this section, we present the framework of our off-policy Inverse Delayed Reinforcement Learning (IDRL) approach. We begin by introducing the overall structure of the framework and provide a detailed explanation of the adversarial formulation for the reward function, along with the underlying intuition and adaption to the off-policy framework. Following this, we delve into the specifics of the algorithm, including the augmentation of expert trajectories with delayed observations and the policy optimization techniques employed. The overall algorithmic framework can be found in Algorithm 1.

---

### Algorithm 1 Inverse Delayed RL

---

- 1: Obtain expert buffer  $\mathcal{D}_{exp}$ .
  - 2: Initialize policy  $\pi_\Delta^\psi$ , discriminator  $D_\theta$ , and buffers  $\mathcal{D}_{env}$ .
  - 3: **for** step  $t$  in  $\{1, \dots, N\}$  **do**
  - 4:   Interact with real environments and add augmented state-action pair  $(x_t, a_t, x_{t+1})$  to  $\mathcal{D}_{env}$ .
  - 5:   Sample delayed observation state-action batch  $(s_{t-\Delta}, a_t, s_{t-\Delta+1}, \dots)$  from  $\mathcal{D}_{exp}$ .
  - 6:   Augment delayed state and action sequences into augmented state action batch  $(x_t, a_t, x_{t+1})$ .
  - 7:   Train  $D_\theta$  via Equation (9) to classify expert samples from  $\mathcal{D}_{exp}$  and samples from  $\mathcal{D}_{env}$ .
  - 8:   Sample new augmented state action batch from  $\mathcal{D}_{env}$ .
  - 9:   Freeze  $\theta$  and calculate rewards of the new augmented state action batch using Equation (10).
  - 10:   Conduct policy optimization procedure Algorithm 2 with calculated rewards to update  $\psi$ .
  - 11: **end for**
-

**Adversarial Formulation.** Generative Adversarial Networks (GANs) (Goodfellow et al., 2020) inspire our adversarial framework, where a binary discriminator  $D_\theta(x_t, a_t)$  is trained to distinguish between augmented state-action samples from expert demonstrations and those generated by the imitator policy  $\pi_\Delta$ , where  $D_\theta$  has the following form:

$$D_\theta(x, a) = \frac{\exp(R_\theta(x, a))}{\exp(R_\theta(x, a)) + \pi_\Delta(a|x)}, \quad (8)$$

where  $R_\theta$  is a multilayer perceptron (MLP) parameterized by  $\theta$  and can be interpreted as the reward used with little modification introduced in the next paragraph. In this context, the imitator policy  $\pi_\Delta$  serves as a generator, improving itself to "fool" the discriminator by making its generated samples indistinguishable from expert samples. The discriminator is trained using the following cross-entropy loss, designed to classify samples as either coming from the expert or the imitation policy:

$$\mathcal{L}_{disc} = -\mathbb{E}_{\mathcal{D}_{exp}} [\log D_\theta(x, a)] - \underbrace{\mathbb{E}_{\pi_\Delta} [\log(1 - D_\theta(x, a))]}_A.$$

The proof of state-action occupancy match between the policy induced from the above adversarial formulation and expert policy have been shown by Ho and Ermon (2016) under the on-policy fashion. The proof sketch should be similar to our modified adversarial formulation with an extension to the augmented state. In the following, we elaborate on the extension to off-policy setting and additional loss terms introduced to stabilize GAN training. To enable an off-policy fashion, importance sampling must be applied to the second term  $A$ , resulting in  $\mathbb{E}_{\pi_\Delta} \left[ \frac{p_{\pi_\Delta}^\omega(x, a)}{p_{\pi_\Delta}(x, a)} \log(1 - D_\theta(x, a)) \right]$ . However, estimating this density ratio is computationally challenging. Additionally, omitting this term has been observed to improve the algorithm's performance in practice, potentially due to reduced gradient variance during updates (Neal, 2001). Despite this improvement, training using cross-entropy loss alone often results in instability due to the complex interaction between the discriminator and the generator policy, which is also updated every iteration. To address these issues, we incorporate additional regularization terms: a gradient penalty  $\mathcal{L}_{grad}$  and an entropy regularization term  $\mathcal{L}_{entropy}$ . These modifications help stabilize training by preventing excessively large gradient updates per training epoch (Nagarajan and Kolter, 2017; Arjovsky et al., 2017). The final loss function for the discriminator is defined as:

$$\mathcal{L}_{disc} = -\mathbb{E}_{\mathcal{D}_{exp}} [\log D_\theta(x, a)] - \mathbb{E}_{\mathcal{D}_{gen}} [\log(1 - D_\theta(x, a))] + \mathcal{L}_{grad} + \mathcal{L}_{entropy}. \quad (9)$$

**Policy Optimization.** In this section, we introduce the reward function derived from the discriminator  $D$  and the policy optimization method used to improve policy in each iteration. To extract the reward signal from the discriminator for each policy update, we use the following formula:

$$\hat{R}_\theta(x, a) = \log(D_\theta(x, a) + \delta) - \log(1 - D_\theta(x, a) + \delta), \quad (10)$$

where  $\delta$  is a marginal constant to prevent numerical error in computation. After derivation  $\hat{R}_\theta$  resembles policy entropy regularized reward for soft policy update, which can be used to satisfy the delayed RL objectives  $\max \mathbb{E}_{\tau_\Delta \sim p(\tau_\Delta)} \left[ \sum_{t=0}^{\tau_\Delta-1} \gamma^t R_\theta(\tau_\Delta) - H(\pi_\Delta) \right]$  (Haarnoja et al., 2018). To update policy  $\pi_\Delta$  for each iteration, we also apply the augmented approach introduced in Section 2. However, using state augmentation for both reward learning and policy optimization is sample inefficient. Thus, we apply the auxiliary delayed RL approach, which learns a value function for short delays and uses bootstrapping and policy improvement techniques to adjust it for long delays (Wu et al., 2024a). The detailed version of the algorithm can be found in Appendix C.

## 6. Experiment

In this section, we evaluate the performance of our Off-Policy Inverse Delayed RL framework. We aim to demonstrate the capability of our method to recover expert behaviors under delayed settings. All experiments are conducted on the MuJoCo benchmarks (Todorov et al., 2012). All the **expert trajectories** are collected by an expert agent trained with VDPO (Wu et al., 2024b) under MuJoCo environments with **5, 10, and 25 delay steps**. We compare our approach with the on-policy algorithms AIRL (Fu et al., 2017), behavior cloning (Torabi et al., 2018), and the off-policy method Discriminator Actor-Critic (DAC) (Kostrikov et al., 2018) based on delayed observation states. For policy optimization to IRL approaches, we use Proximal Policy Optimization (PPO) (Schulman et al., 2017) for AIRL, and Soft Actor-Critic (SAC) (Haarnoja et al., 2018) for DAC. All implementations of PPO and SAC are referenced from the Clean RL library (Huang et al., 2022). Each algorithm is trained with 100k environmental steps and evaluated each 1k steps across 5 different seeds for `InvertedPendulum-v4`. For `Hopper-v4`, `HalfCheetah-v4`, `Walker2d-v4`, and `Ant-v4`, AIRL is trained with 10M steps and evaluated every 100k steps across 5 different seeds, but DAC and our algorithm are trained with 1M environmental steps and evaluated every 10k steps across 5 different seeds. We conduct the aforementioned series of experiments under **various numbers of expert trajectories ranging from 10 to 1000**. All the experiments are run on the Desktop equipped with RTX 4090 and Core-i9 13900K. Training graphs are provided in Appendix B. Across different scenarios, we showcase our method’s efficacy in two dimensions.

- **Performance Superiority:** Our method consistently outperforms baseline approaches in recovering expert behaviors across various environments, even under diverse delay-length settings. When expert demonstrations are sufficient, our method achieves near-complete recovery of expert performance, whereas most baselines fail to learn meaningful policies.
- **Robust Utilization of Limited Expert Demonstrations:** Even with limited expert demonstrations, our method demonstrates the ability to recover a reasonable policy, outperforming baselines that struggle to reproduce expert behaviors in most environments.

### 6.1. Impact of Varying Delays

We investigate the effect of varying delays (5, 10, and 25 delay steps) on performance, using 1000 expert demonstration trajectories. Detailed learning curves in Appendix B support our findings. As shown in Table 1, our IDRL framework consistently outperforms baseline methods (AIRL, DAC, and BC) across all tested MuJoCo environments. Notably, as delays increase, the performance of the expert policy deteriorates, leading to noisier expert trajectories and a corresponding decline in baseline performance. While baseline methods exhibit significant degradation or fail entirely in certain environments, IDRL maintains near-expert performance across all delay conditions, demonstrating remarkable robustness. This resilience is particularly evident in complex environments like `Ant-v4` and `Walker2d-v4`, where IDRL consistently achieves superior performance, whereas DAC and AIRL fail to adapt. BC can recover part of the expert behaviors, but still a large margin below ours. These advantages are even more notable in the low dimensional task (`InvertedPendulum-v4`) and medium dimensional tasks (`Hopper-v4` and `HalfCheetah-v4`). IDRL’s robustness stems from its augmented state representation, which enriches the feature space to better capture delayed dependencies, combined with advanced policy optimization techniques that mitigate the adverse



Table 1: Performance comparison across environments and algorithms with 1000 expert demonstration trajectories under varying delay steps from 5 to 25. Results are mean  $\pm$  standard deviation. Best performances are highlighted in blue. We omit InvertedPendulum-v4 under 25 delays, since the expert policy degrades to performance near random policy.

Task	Delay	Expert	BC	AIRL	DAC	IDRL (Ours)
InvertedPendulum-v4	5	974.29 $\pm$ 157.44	15.27 $\pm$ 2.11	28.93 $\pm$ 5.28	27.80 $\pm$ 20.28	1000.00 $\pm$ 0.00
	10	681.11 $\pm$ 462.73	21.06 $\pm$ 6.16	28.53 $\pm$ 1.59	23.00 $\pm$ 7.72	867.87 $\pm$ 186.87
Hopper-v4	5	3738.91 $\pm$ 34.63	176.67 $\pm$ 43.35	203.26 $\pm$ 113.29	516.88 $\pm$ 364.13	3569.99 $\pm$ 44.33
	10	3492.25 $\pm$ 239.45	14.15 $\pm$ 4.46	182.52 $\pm$ 50.31	120.28 $\pm$ 60.35	3321.84 $\pm$ 50.74
	25	2107.44 $\pm$ 1399.19	101.32 $\pm$ 50.67	182.64 $\pm$ 11.02	96.96 $\pm$ 15.06	1814.18 $\pm$ 756.36
HalfCheetah-v4	5	5451.92 $\pm$ 239.91	2384.60 $\pm$ 563.00	0.05 $\pm$ 0.11	-220.04 $\pm$ 285.61	4561.01 $\pm$ 313.91
	10	4986.07 $\pm$ 852.61	793.87 $\pm$ 973.06	0.05 $\pm$ 0.12	-234.68 $\pm$ 85.08	5061.02 $\pm$ 154.63
	25	4088.53 $\pm$ 1600.44	1087.04 $\pm$ 319.38	0.05 $\pm$ 0.13	-225.55 $\pm$ 146.12	3256.81 $\pm$ 693.51
Walker2d-v4	5	4124.08 $\pm$ 1289.46	1039.87 $\pm$ 389.39	146.64 $\pm$ 45.33	812.51 $\pm$ 176.26	4424.19 $\pm$ 138.03
	10	4491.65 $\pm$ 610.81	763.85 $\pm$ 767.61	136.87 $\pm$ 99.16	315.09 $\pm$ 436.99	4283.64 $\pm$ 105.36
	25	1955.69 $\pm$ 1458.62	604.07 $\pm$ 277.71	115.31 $\pm$ 27.66	60.91 $\pm$ 72.40	1437.88 $\pm$ 506.97
Ant-v4	5	5281.73 $\pm$ 1627.50	761.11 $\pm$ 107.30	1003.40 $\pm$ 2.09	-52.27 $\pm$ 12.55	5764.42 $\pm$ 71.72
	10	3618.59 $\pm$ 868.75	799.43 $\pm$ 138.88	1004.32 $\pm$ 1.10	-62.64 $\pm$ 6.27	3949.62 $\pm$ 31.93
	25	3432.42 $\pm$ 580.22	698.95 $\pm$ 20.66	1003.21 $\pm$ 3.04	-40.43 $\pm$ 27.07	3024.53 $\pm$ 150.83

effects of delays. These results empirically validate our theoretical analysis, highlighting the effectiveness of leveraging augmented state representations over direct delayed observations in handling delay-affected environments. We also observe randomness in the performance of some algorithms under certain scenarios, likely due to their inability to extract meaningful reward features from expert demonstrations. Additionally, BC exhibits inconsistent performance trends in some environments. Since BC directly replicates the action distribution of expert demonstrations, any noise present in the expert trajectories—potentially introduced during data collection—can severely degrade the imitator’s performance.

## 6.2. Quantity of Expert Demonstrations

We analyze the impact of the quantity of expert demonstrations on training performance under a moderate 10 delay steps, with results summarized in Table 2. Across all methods, an overall increasing trend in return value is observed as the number of expert trajectories increases (10, 100, and 1000). In InvertedPendulum-v4, IDRL consistently performs at the expert level with performance increases according to the increase in quantity of expert demonstrations, demonstrating its resilience and efficiency regardless of the number of expert trajectories, while all the other baselines fail to recover meaningful expert behaviors. In Hopper-v4, IDRL similarly scales to expert-level performance as the quantity of demonstrations increases. Though there are notable gaps with different available quantity of expert demonstrations, our method still outperforms all baselines even with fewer demonstrations. We can observe a similar trend in Walker2d-v4, where our method also possesses a significant performance margin compared to all the other baselines. While BC initially outperforms IDRL with limited demonstrations (10 and 100 trajectories) in HalfCheetah-v4, IDRL demonstrates superior scalability as more expert data becomes available. With 1000 trajectories,

Table 2: Performance comparison across different environments and algorithms with a 10 delay steps under varying quantity of expert trajectories from 10 to 1000. Results are mean  $\pm$  standard deviation. Best performances are highlighted in blue.

Task	#Traj	Expert	BC	AIRL	DAC	IDRL (Ours)
InvertedPendulum-v4	10	406.40 $\pm$ 484.67	25.77 $\pm$ 3.39	29.13 $\pm$ 2.88	21.47 $\pm$ 4.22	934.07 $\pm$ 93.24
	100	673.29 $\pm$ 465.53	23.38 $\pm$ 4.51	28.73 $\pm$ 4.07	27.07 $\pm$ 5.01	802.13 $\pm$ 161.59
	1000	681.11 $\pm$ 462.73	21.06 $\pm$ 6.16	28.53 $\pm$ 1.59	23.00 $\pm$ 7.72	867.87 $\pm$ 186.87
Hopper-v4	10	3567.45 $\pm$ 64.08	149.31 $\pm$ 21.43	198.56 $\pm$ 59.59	114.83 $\pm$ 89.47	1008.50 $\pm$ 12.30
	100	3497.54 $\pm$ 193.82	125.04 $\pm$ 48.81	188.51 $\pm$ 64.77	99.21 $\pm$ 36.76	1715.82 $\pm$ 1006.63
	1000	3492.25 $\pm$ 239.45	14.15 $\pm$ 4.46	182.52 $\pm$ 50.31	120.28 $\pm$ 60.35	3321.84 $\pm$ 50.74
HalfCheetah-v4	10	5171.72 $\pm$ 580.66	-58.58 $\pm$ 257.86	0.05 $\pm$ 0.13	-197.25 $\pm$ 209.73	41.28 $\pm$ 70.15
	100	4919.62 $\pm$ 865.51	-17.68 $\pm$ 218.00	0.05 $\pm$ 0.12	-198.83 $\pm$ 67.36	-10.68 $\pm$ 6.06
	1000	4986.07 $\pm$ 852.61	793.87 $\pm$ 973.06	0.05 $\pm$ 0.12	-234.68 $\pm$ 85.08	5061.02 $\pm$ 154.63
Walker2d-v4	10	4578.05 $\pm$ 31.78	142.05 $\pm$ 122.64	145.65 $\pm$ 110.57	342.81 $\pm$ 359.79	1015.10 $\pm$ 76.16
	100	4449.56 $\pm$ 723.44	90.02 $\pm$ 107.01	139.09 $\pm$ 103.83	389.67 $\pm$ 469.74	1146.64 $\pm$ 1002.86
	1000	4491.65 $\pm$ 610.81	763.85 $\pm$ 767.61	136.87 $\pm$ 99.16	315.09 $\pm$ 436.99	4283.64 $\pm$ 105.36
Ant-v4	10	3187.90 $\pm$ 1263.76	758.24 $\pm$ 367.63	1005.22 $\pm$ 0.63	-46.57 $\pm$ 21.93	932.69 $\pm$ 3.28
	100	3598.60 $\pm$ 825.72	848.39 $\pm$ 216.35	1003.04 $\pm$ 1.78	-42.47 $\pm$ 12.48	920.06 $\pm$ 7.74
	1000	3618.59 $\pm$ 868.75	799.43 $\pm$ 138.88	1004.32 $\pm$ 1.10	-62.64 $\pm$ 6.27	3949.62 $\pm$ 31.93

IDRL significantly surpasses all baselines in `HalfCheetah-v4`, highlighting the effectiveness of its augmented state representation in leveraging larger datasets. In `Ant-v4`, BC and our method have competitive performance when demonstrations are limited, but a significant margin when more expert demonstrations become available. These results emphasize that the augmented states employed by IDRL not only enhance scalability towards expert-level performance but also ensure robust learning under delay-affected settings, particularly as the availability of expert data increases.

## 7. Conclusion

In this work, we introduced an Inverse Delayed Reinforcement Learning (IDRL) framework that effectively addresses the challenges of learning from expert demonstrations under delayed settings. By leveraging augmented state representations and advanced policy optimization techniques, our method demonstrated superior performance across a range of environments and delay conditions, consistently outperforming baseline methods. Our empirical results validated the theoretical advantages of using augmented states over direct delayed observations, highlighting the robustness and scalability of IDRL, particularly when faced with varying delays and quantities of expert data. While our approach significantly advances state-of-the-art imitation learning with delays, several avenues for future research remain open. First, extending IDRL to more complex, high-dimensional environments, such as those involving real-world robotics, would further test its robustness and generalizability. Additionally, exploring methods to reduce the dependency on large quantities of expert demonstrations, such as leveraging transfer learning or combining imitation learning with self-supervised approaches, could broaden the applicability of IDRL in data-scarce scenarios. Finally, integrating IDRL with online adaptation mechanisms to dynamically handle non-stationary delays during deployment represents an exciting direction for future work.

## **Acknowledgments**

We thank a bunch of people.

## References

- Eitan Altman and Philippe Nain. Closed-loop control with delayed information. *ACM sigmetrics performance evaluation review*, 20(1):193–204, 1992.
- Jose A Arjona-Medina, Michael Gillhofer, Michael Widrich, Thomas Unterthiner, Johannes Brandstetter, and Sepp Hochreiter. Rudder: Return decomposition for delayed rewards. *Advances in Neural Information Processing Systems*, 32, 2019.
- Martin Arjovsky, Soumith Chintala, and Léon Bottou. Wasserstein generative adversarial networks. In *International conference on machine learning*, pages 214–223. PMLR, 2017.
- Saurabh Arora and Prashant Doshi. A survey of inverse reinforcement learning: Challenges, methods and progress. *Artificial Intelligence*, 297:103500, 2021.
- Christopher Berner, Greg Brockman, Brooke Chan, Vicki Cheung, Przemyslaw Dkebiak, Christy Dennison, David Farhi, Quirin Fischer, Shariq Hashme, Chris Hesse, et al. Dota 2 with large scale deep reinforcement learning. *arXiv preprint arXiv:1912.06680*, 2019.
- Lionel Blondé and Alexandros Kalousis. Sample-efficient imitation learning via generative adversarial nets. In *The 22nd International Conference on Artificial Intelligence and Statistics*, pages 3138–3148. PMLR, 2019.
- Daniel Brown, Wonjoon Goo, Prabhat Nagarajan, and Scott Niekum. Extrapolating beyond sub-optimal demonstrations via inverse reinforcement learning from observations. In *International conference on machine learning*, pages 783–792. PMLR, 2019.
- Zhiguang Cao, Hongliang Guo, Wen Song, Kaizhou Gao, Zhenghua Chen, Le Zhang, and Xuexi Zhang. Using reinforcement learning to minimize the probability of delay occurrence in transportation. *IEEE transactions on vehicular technology*, 69(3):2424–2436, 2020.
- Alex J Chan and Mihaela van der Schaar. Scalable bayesian inverse reinforcement learning. *arXiv preprint arXiv:2102.06483*, 2021.
- Baiming Chen, Mengdi Xu, Liang Li, and Ding Zhao. Delay-aware model-based reinforcement learning for continuous control. *Neurocomputing*, 450:119–128, 2021.
- Jaedeug Choi and Kee-Eung Kim. Map inference for bayesian inverse reinforcement learning. *Advances in neural information processing systems*, 24, 2011.
- Felipe Codevilla, Matthias Müller, Antonio López, Vladlen Koltun, and Alexey Dosovitskiy. End-to-end driving via conditional imitation learning. In *2018 IEEE international conference on robotics and automation (ICRA)*, pages 4693–4700. IEEE, 2018.
- Shenghua Feng, Mingshuai Chen, Naijun Zhan, Martin Fränzle, and Bai Xue. Taming delays in dynamical systems: Unbounded verification of delay differential equations. In *International Conference on Computer Aided Verification*, pages 650–669. Springer, 2019.
- Chelsea Finn, Sergey Levine, and Pieter Abbeel. Guided cost learning: Deep inverse optimal control via policy optimization. In *International conference on machine learning*, pages 49–58. PMLR, 2016.

- Justin Fu, Katie Luo, and Sergey Levine. Learning robust rewards with adversarial inverse reinforcement learning. *arXiv preprint arXiv:1710.11248*, 2017.
- Ian Goodfellow, Jean Pouget-Abadie, Mehdi Mirza, Bing Xu, David Warde-Farley, Sherjil Ozair, Aaron Courville, and Yoshua Bengio. Generative adversarial networks. *Communications of the ACM*, 63(11):139–144, 2020.
- Tuomas Haarnoja, Aurick Zhou, Pieter Abbeel, and Sergey Levine. Soft actor-critic: Off-policy maximum entropy deep reinforcement learning with a stochastic actor. In *International conference on machine learning*, pages 1861–1870. PMLR, 2018.
- Beining Han, Zhizhou Ren, Zuofan Wu, Yuan Zhou, and Jian Peng. Off-policy reinforcement learning with delayed rewards. In *International Conference on Machine Learning*, pages 8280–8303. PMLR, 2022.
- Joel Hasbrouck and Gideon Saar. Low-latency trading. *Journal of Financial Markets*, 16(4):646–679, 2013.
- Andreas B Hempel, Paul J Goulart, and John Lygeros. Inverse parametric optimization with an application to hybrid system control. *IEEE Transactions on automatic control*, 60(4):1064–1069, 2014.
- Jonathan Ho and Stefano Ermon. Generative adversarial imitation learning. *Advances in neural information processing systems*, 29, 2016.
- Shengyi Huang, Rousslan Fernand Julien Dossa, Chang Ye, Jeff Braga, Dipam Chakraborty, Kinal Mehta, and Jo go GM Ara sjo. Cleanrl: High-quality single-file implementations of deep reinforcement learning algorithms. *Journal of Machine Learning Research*, 23(274):1–18, 2022.
- Jemin Hwangbo, Inkyu Sa, Roland Siegwart, and Marco Hutter. Control of a quadrotor with reinforcement learning. *IEEE Robotics and Automation Letters*, 2(4):2096–2103, 2017.
- Rudolf Emil Kalman. When is a linear control system optimal? 1964.
- Armin Karamzade, Kyungmin Kim, Montek Kalsi, and Roy Fox. Reinforcement learning from delayed observations via world models. *Reinforcement Learning Journal*, 2024.
- Konstantinos V Katsikopoulos and Sascha E Engelbrecht. Markov decision processes with delays and asynchronous cost collection. *IEEE transactions on automatic control*, 48(4):568–574, 2003a.
- Konstantinos V Katsikopoulos and Sascha E Engelbrecht. Markov decision processes with delays and asynchronous cost collection. *IEEE transactions on automatic control*, 48(4):568–574, 2003b.
- Jangwon Kim, Hangeol Kim, Jiwook Kang, Jongchan Baek, and Soohye Han. Belief projection-based reinforcement learning for environments with delayed feedback. In *Thirty-seventh Conference on Neural Information Processing Systems*, 2023.
- Edouard Klein, Matthieu Geist, Bilal Piot, and Olivier Pietquin. Inverse reinforcement learning through structured classification. *Advances in neural information processing systems*, 25, 2012.

- Petar Kormushev, Sylvain Calinon, and Darwin G Caldwell. Reinforcement learning in robotics: Applications and real-world challenges. *Robotics*, 2(3):122–148, 2013.
- Ilya Kostrikov, Kumar Krishna Agrawal, Debidatta Dwibedi, Sergey Levine, and Jonathan Tompson. Discriminator-actor-critic: Addressing sample inefficiency and reward bias in adversarial imitation learning. *arXiv preprint arXiv:1809.02925*, 2018.
- Sanjay Krishnan, Animesh Garg, Richard Liaw, Lauren Miller, Florian T Pokorny, and Ken Goldberg. Hirl: Hierarchical inverse reinforcement learning for long-horizon tasks with delayed rewards. *arXiv preprint arXiv:1604.06508*, 2016.
- Sanjay Krishnan, Animesh Garg, Richard Liaw, Brijen Thananjeyan, Lauren Miller, Florian T Pokorny, and Ken Goldberg. Swirl: A sequential windowed inverse reinforcement learning algorithm for robot tasks with delayed rewards. *The international journal of robotics research*, 38(2-3):126–145, 2019.
- Sergey Levine, Zoran Popovic, and Vladlen Koltun. Feature construction for inverse reinforcement learning. *Advances in neural information processing systems*, 23, 2010.
- Sergey Levine, Zoran Popovic, and Vladlen Koltun. Nonlinear inverse reinforcement learning with gaussian processes. *Advances in neural information processing systems*, 24, 2011.
- Pierre Liotet, Erick Venneri, and Marcello Restelli. Learning a belief representation for delayed reinforcement learning. In *2021 International Joint Conference on Neural Networks (IJCNN)*, pages 1–8. IEEE, 2021.
- Pierre Liotet, Davide Maran, Lorenzo Bisi, and Marcello Restelli. Delayed reinforcement learning by imitation. In *International Conference on Machine Learning*, pages 13528–13556. PMLR, 2022.
- Wenyou Liu, Yunjun Bai, Li Jiao, and Naijun Zhan. Safety guarantee for time-delay systems with disturbances. *Science China Information Sciences*, 66(3):132102, 2023.
- A Rupam Mahmood, Dmytro Korenkevych, Brent J Komer, and James Bergstra. Setting up a reinforcement learning task with a real-world robot. In *2018 IEEE/RSJ International Conference on Intelligent Robots and Systems (IROS)*, pages 4635–4640. IEEE, 2018.
- Alberto Maria Metelli, Flavio Mazzolini, Lorenzo Bisi, Luca Sabbioni, and Marcello Restelli. Control frequency adaptation via action persistence in batch reinforcement learning. In *International Conference on Machine Learning*, pages 6862–6873. PMLR, 2020.
- Vaishnavh Nagarajan and J Zico Kolter. Gradient descent gan optimization is locally stable. *Advances in neural information processing systems*, 30, 2017.
- Radford M Neal. Annealed importance sampling. *Statistics and computing*, 11:125–139, 2001.
- Andrew Y Ng, Stuart Russell, et al. Algorithms for inverse reinforcement learning. In *Icml*, volume 1, page 2, 2000.
- Xue Bin Peng, Erwin Coumans, Tingnan Zhang, Tsang-Wei Lee, Jie Tan, and Sergey Levine. Learning agile robotic locomotion skills by imitating animals. *arXiv preprint arXiv:2004.00784*, 2020.

- Emmanuel Rachelson and Michail G Lagoudakis. On the locality of action domination in sequential decision making. 2010.
- Deepak Ramachandran and Eyal Amir. Bayesian inverse reinforcement learning. In *IJCAI*, volume 7, pages 2586–2591, 2007.
- Stuart Russell. Learning agents for uncertain environments. In *Proceedings of the eleventh annual conference on Computational learning theory*, pages 101–103, 1998.
- John Schulman, Filip Wolski, Prafulla Dhariwal, Alec Radford, and Oleg Klimov. Proximal policy optimization algorithms. *arXiv preprint arXiv:1707.06347*, 2017.
- John Shore and Rodney Johnson. Axiomatic derivation of the principle of maximum entropy and the principle of minimum cross-entropy. *IEEE Transactions on information theory*, 26(1):26–37, 1980.
- David Silver, Julian Schrittwieser, Karen Simonyan, Ioannis Antonoglou, Aja Huang, Arthur Guez, Thomas Hubert, Lucas Baker, Matthew Lai, Adrian Bolton, et al. Mastering the game of go without human knowledge. *nature*, 550(7676):354–359, 2017.
- Han Su, Shenghua Feng, Sinong Zhan, and Naijun Zhan. Switching controller synthesis for hybrid systems against stl formulas. In *International Symposium on Formal Methods*, pages 229–247. Springer, 2024.
- Wei Sun, Yanjun Chen, Simon Zhan, Teng Han, Feng Tian, Hongan Wang, and Xing-Dong Yang. Relectrode: A reconfigurable electrode for multi-purpose sensing based on microfluidics. In *Proceedings of the 2021 CHI Conference on Human Factors in Computing Systems*, pages 1–12, 2021.
- Wei Sun, Yuwen Chen, Yanjun Chen, Xiaopeng Zhang, Simon Zhan, Yixin Li, Jiecheng Wu, Teng Han, Haipeng Mi, Jingxian Wang, et al. Microfluid: A multi-chip rfid tag for interaction sensing based on microfluidic switches. *Proceedings of the ACM on Interactive, Mobile, Wearable and Ubiquitous Technologies*, 6(3):1–23, 2022.
- Emanuel Todorov, Tom Erez, and Yuval Tassa. Mujoco: A physics engine for model-based control. In *2012 IEEE/RSJ international conference on intelligent robots and systems*, pages 5026–5033. IEEE, 2012.
- Faraz Torabi, Garrett Warnell, and Peter Stone. Generative adversarial imitation from observation. *arXiv preprint arXiv:1807.06158*, 2018.
- David Valensi, Esther Derman, Shie Mannor, and Gal Dalal. Tree search-based policy optimization under stochastic execution delay. *arXiv preprint arXiv:2404.05440*, 2024.
- Cédric Villani et al. *Optimal transport: old and new*, volume 338. Springer, 2009.
- Aladin Virmaux and Kevin Scaman. Lipschitz regularity of deep neural networks: analysis and efficient estimation. *Advances in Neural Information Processing Systems*, 31, 2018.

- Thomas J Walsh, Ali Nouri, Lihong Li, and Michael L Littman. Learning and planning in environments with delayed feedback. *Autonomous Agents and Multi-Agent Systems*, 18:83–105, 2009.
- Yixuan Wang, Simon Zhan, Zhilu Wang, Chao Huang, Zhaoran Wang, Zhuoran Yang, and Qi Zhu. Joint differentiable optimization and verification for certified reinforcement learning. In *Proceedings of the ACM/IEEE 14th International Conference on Cyber-Physical Systems (with CPS-IoT Week 2023)*, pages 132–141, 2023a.
- Yixuan Wang, Simon Sinong Zhan, Ruochen Jiao, Zhilu Wang, Wanxin Jin, Zhuoran Yang, Zhaoran Wang, Chao Huang, and Qi Zhu. Enforcing hard constraints with soft barriers: Safe reinforcement learning in unknown stochastic environments. In *International Conference on Machine Learning*, pages 36593–36604. PMLR, 2023b.
- Qingyuan Wu, Simon Sinong Zhan, Yixuan Wang, Chung-Wei Lin, Chen Lv, Qi Zhu, and Chao Huang. Boosting long-delayed reinforcement learning with auxiliary short-delayed task. *arXiv preprint arXiv:2402.03141*, 2024a.
- Qingyuan Wu, Simon Sinong Zhan, Yixuan Wang, Yuhui Wang, Chung-Wei Lin, Chen Lv, Qi Zhu, and Chao Huang. Variational delayed policy optimization. *arXiv preprint arXiv:2405.14226*, 2024b.
- Markus Wulfmeier, Peter Ondruska, and Ingmar Posner. Maximum entropy deep inverse reinforcement learning. *arXiv preprint arXiv:1507.04888*, 2015.
- Minzhi Xie, Bo Xia, Yalou Yu, Xueqian Wang, and Yongzhe Chang. Addressing delays in reinforcement learning via delayed adversarial imitation learning. In *International Conference on Artificial Neural Networks*, pages 271–282. Springer, 2023.
- Bai Xue, Peter Nazier Mosaad, Martin Fränzle, Mingshuai Chen, Yangjia Li, and Naijun Zhan. Safe over-and under-approximation of reachable sets for delay differential equations. In *Formal Modeling and Analysis of Timed Systems: 15th International Conference, FORMATS 2017, Berlin, Germany, September 5–7, 2017, Proceedings 15*, pages 281–299. Springer, 2017.
- Bai Xue, Qiuye Wang, Shenghua Feng, and Naijun Zhan. Over-and underapproximating reach sets for perturbed delay differential equations. *IEEE Transactions on Automatic Control*, 66(1): 283–290, 2020.
- S. S. Zhan, Q. Wu, P. Wang, Y. Wang, R. Jiao, C. Huang, and Q. Zhu. Model-based reward shaping for adversarial inverse reinforcement learning in stochastic environments. *arXiv preprint arXiv:2410.03847*, 2024a.
- Sinong Zhan, Yixuan Wang, Qingyuan Wu, Ruochen Jiao, Chao Huang, and Qi Zhu. State-wise safe reinforcement learning with pixel observations. In *6th Annual Learning for Dynamics & Control Conference*, pages 1187–1201. PMLR, 2024b.
- Yuyang Zhang, Runyu Zhang, Yuantao Gu, and Na Li. Multi-agent reinforcement learning with reward delays. In *Learning for Dynamics and Control Conference*, pages 692–704. PMLR, 2023.



Brian D Ziebart, Andrew L Maas, J Andrew Bagnell, Anind K Dey, et al. Maximum entropy inverse reinforcement learning. In *Aaai*, volume 8, pages 1433–1438. Chicago, IL, USA, 2008.

Brian D Ziebart, J Andrew Bagnell, and Anind K Dey. Modeling interaction via the principle of maximum causal entropy. 2010.

## Appendix A. Proof

**Lemma 6 (Time Lipschitz Continuous Belief)** *Given a  $L_{\mathcal{R}}$ -Time Lipschitz Continuous Dynamic, the belief  $b$  is  $L_{\mathcal{R}}$ -Time Lipschitz Continuous,  $\forall x_t \in \mathcal{X}$ , satisfying*

$$W_1(b(\cdot|x_t)||\delta_{s_{t-\Delta}}) \leq \Delta L_{\mathcal{T}}.$$

**Proof** We denote that  $b^{(\Delta)}(\cdot|x_t) = b(\cdot|x_t)$  and  $b^{(1)}(\cdot|x_t) = \mathcal{T}(\cdot|s_{t-\Delta}, a_{t-\Delta})$ .

$$\begin{aligned} W_1(b(\cdot|x_t)||\delta_{s_{t-\Delta}}) &\leq W_1(b^{(\Delta)}(\cdot|x_t)||b^{(\Delta-1)}(\cdot|x_t)) + W_1(b^{(\Delta-1)}(\cdot|x_t)||\delta_{s_{t-\Delta}}) \\ &\leq L_{\mathcal{T}} + W_1(b^{(\Delta-1)}(\cdot|x_t)||b^{(\Delta-2)}(\cdot|x_t)) + W_1(b^{(\Delta-2)}(\cdot|x_t)||\delta_{s_{t-\Delta}}) \\ &\dots \\ &\leq (\Delta - 1)L_{\mathcal{T}} + W_1(b^{(1)}(\cdot|x_t)||\delta_{s_{t-\Delta}}) \\ &\leq \Delta L_{\mathcal{T}} \end{aligned}$$

■

**Lemma 7 (Reward Delayed Difference Upper Bound)** *Given a  $L_{\mathcal{R}}$ -Time Lipschitz Continuous Dynamic and  $L_{\mathcal{R}}$ -Lipschitz Continuous Reward function,  $\forall x_t \in \mathcal{X}$ , the upper bound of reward delayed difference is as follows:*

$$d_{\mathcal{R}} \left( \mathbb{E}_{s_t \sim b(\cdot|x_t)} [\mathcal{R}(s_t, a_t)] - \mathcal{R}(s_{t-\Delta}, a_t) \right) \leq \Delta L_{\mathcal{R}} L_{\mathcal{T}}$$

**Proof** We substitute the delayed reward function  $R_{\Delta}(x_t, a_t)$  to the belief version  $\mathcal{E}_{s_t \sim b(\cdot|x_t)}[R(s_t, a_t)]$

$$\begin{aligned} d_{\mathcal{R}} \left( \mathbb{E}_{s_t \sim b(\cdot|x_t)} [\mathcal{R}(s_t, a_t)] - \mathcal{R}(s_{t-\Delta}, a_t) \right) &\leq L_{\mathcal{R}} \mathbb{E}_{s_t \sim b(\cdot|x_t)} [d_{\mathcal{S}}(s_t, s_{t-\Delta})] \\ &\leq L_{\mathcal{R}} W_1(b(\cdot|x_t)||\delta_{s_{t-\Delta}}) \\ &\leq \Delta L_{\mathcal{R}} L_{\mathcal{T}}. \end{aligned}$$

■

**Proposition 8 (Performance Difference Upper Bound)** *Given a  $L_{\mathcal{R}}$ -Time Lipschitz Continuous Dynamic,  $L_{\mathcal{R}}$ -Lipschitz Continuous Reward function, and policies  $\pi$  and  $\pi_{\Delta}$ ,  $\forall x_t \in \mathcal{X}$ , the upper bound of performance difference is as follows:*

$$\|V^{\pi_{\Delta}}(x_t) - V^{\pi}(x_t)\| \leq \frac{1}{1-\gamma} [R_{\max} + \Delta L_{\mathcal{R}} L_{\mathcal{T}}]$$

**Proof**

$$\begin{aligned}
 & V^{\pi\Delta}(x_t) - V^\pi(x_t) \\
 = & V^{\pi\Delta}(x_t) - \mathbb{E}_{\substack{x_{t+1} \sim \mathcal{T}_\Delta(\cdot|x_t, a_t) \\ a_t \sim \pi(\cdot|x_t)}} \left[ \mathbb{E}_{s_t \sim b(\cdot|x_t)} [\mathcal{R}(s_t, a_t)] + \gamma V^{\pi\Delta}(x_{t+1}) \right] \\
 & + \mathbb{E}_{\substack{x_{t+1} \sim \mathcal{T}_\Delta(\cdot|x_t, a_t) \\ a_t \sim \pi(\cdot|x_t)}} \left[ \mathbb{E}_{s_t \sim b(\cdot|x_t)} [\mathcal{R}(s_t, a_t)] + \gamma V^{\pi\Delta}(x_{t+1}) \right] - V^\pi(x_t) \\
 = & V^{\pi\Delta}(x_t) - \mathbb{E}_{a_t \sim \pi(\cdot|x_t)} [Q^{\pi\Delta}(x_t, a_t)] \\
 & + \mathbb{E}_{\substack{x_{t+1} \sim \mathcal{T}_\Delta(\cdot|x_t, a_t) \\ a_t \sim \pi(\cdot|x_t)}} \left[ \mathbb{E}_{s_t \sim b(\cdot|x_t)} [\mathcal{R}(s_t, a_t)] - \mathcal{R}(s_t, a_t) \right] + \gamma \mathbb{E}_{\substack{x_{t+1} \sim \mathcal{T}_\Delta(\cdot|x_t, a_t) \\ a_t \sim \pi(\cdot|x_t)}} [V^{\pi\Delta}(x_{t+1}) - V^\pi(x_{t+1})]
 \end{aligned}$$

Therefore,

$$\begin{aligned}
 & \|V^{\pi\Delta}(x_t) - V^\pi(x_t)\| \\
 \leq & \|V^{\pi\Delta}(x_t) - \mathbb{E}_{a_t \sim \pi(\cdot|x_t)} [Q^{\pi\Delta}(x_t, a_t)]\| \\
 & + \left\| \mathbb{E}_{\substack{x_{t+1} \sim \mathcal{T}_\Delta(\cdot|x_t, a_t) \\ a_t \sim \pi(\cdot|x_t)}} \left[ \mathbb{E}_{s_t \sim b(\cdot|x_t)} [\mathcal{R}(s_t, a_t)] - \mathcal{R}(s_t, a_t) \right] \right\| \\
 & + \gamma \left\| \mathbb{E}_{\substack{x_{t+1} \sim \mathcal{T}_\Delta(\cdot|x_t, a_t) \\ a_t \sim \pi(\cdot|x_t)}} [V^{\pi\Delta}(x_{t+1}) - V^\pi(x_{t+1})] \right\| \\
 \leq & \frac{1}{1-\gamma} [\mathcal{R}_{\max} + \Delta L_{\mathcal{R}} L_{\mathcal{T}}]
 \end{aligned}$$

■

**Appendix B. Learning Curves**

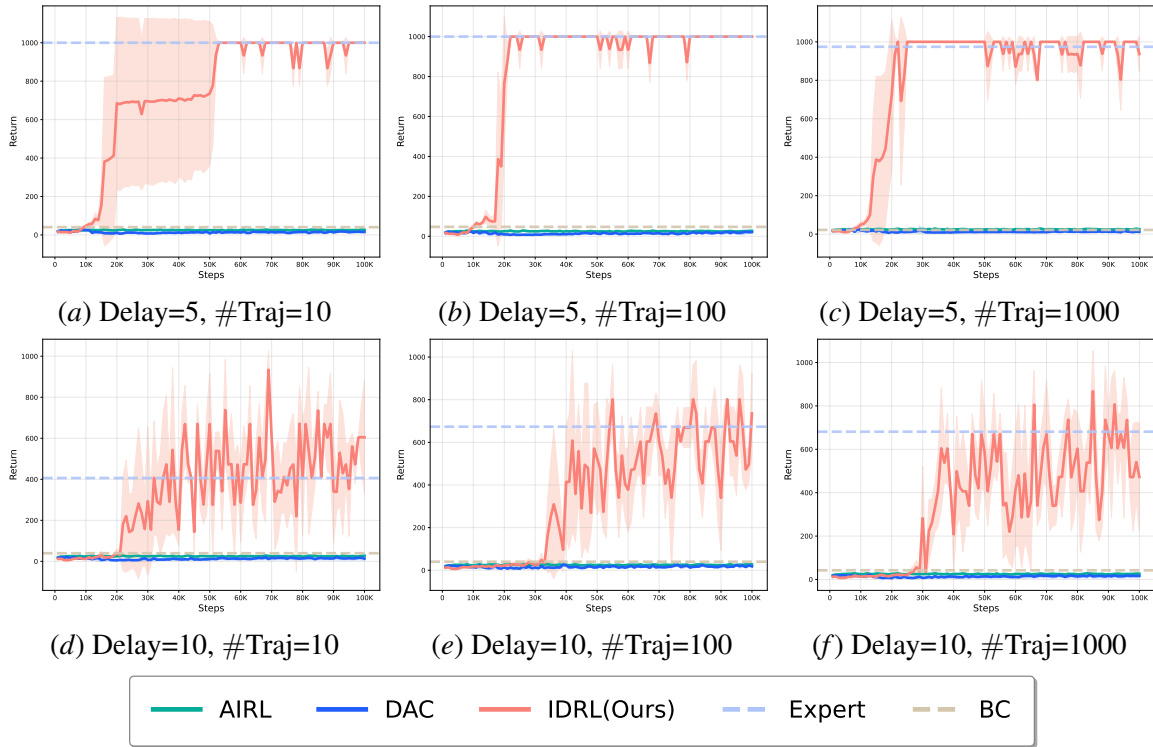


Figure 1: Learning Curves on InvertedPendulum-v4 with different delays and quantities of expert demonstrations.

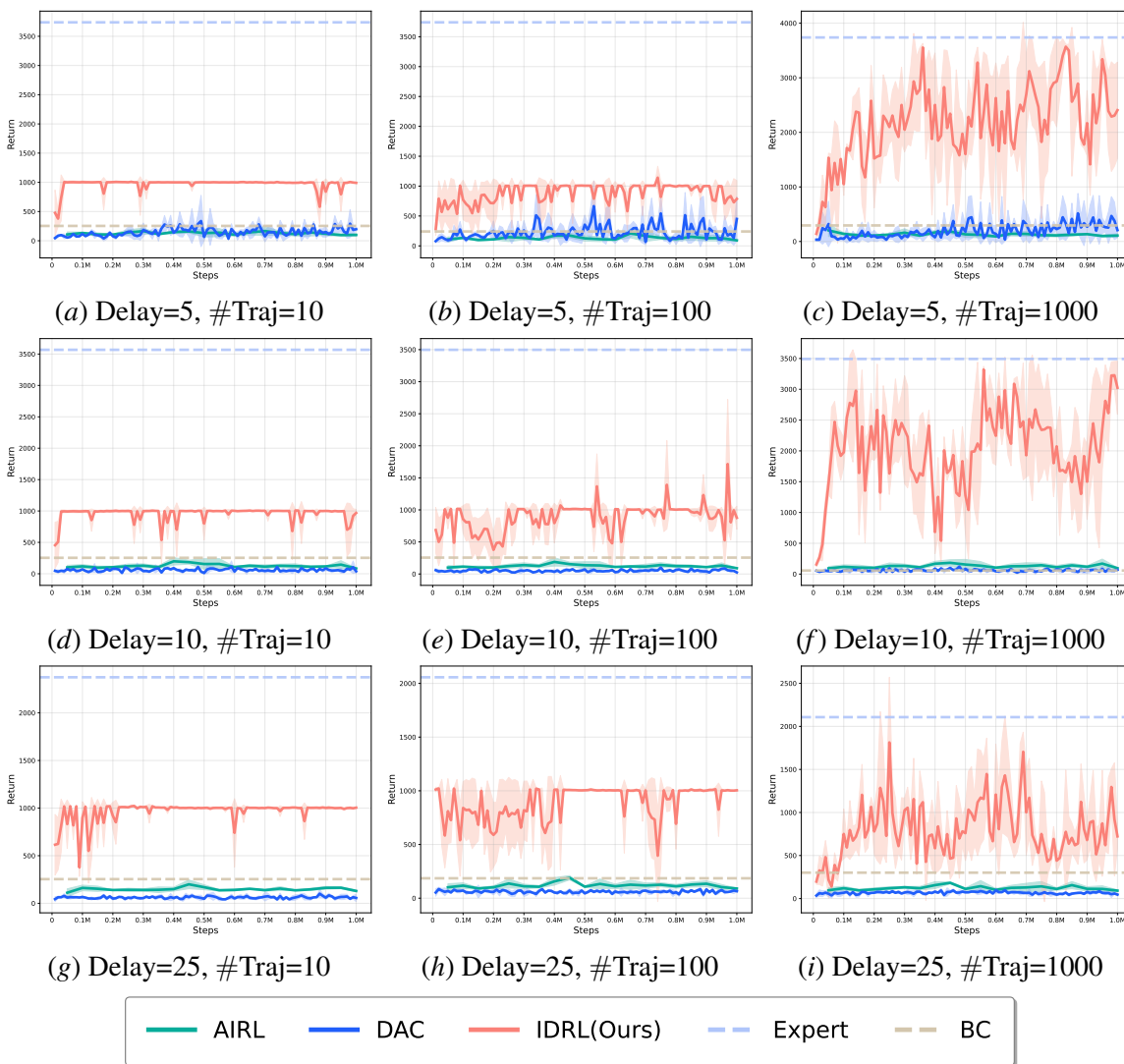


Figure 2: Learning Curves on Hopper-v4 with different delays and quantities of expert demonstrations.

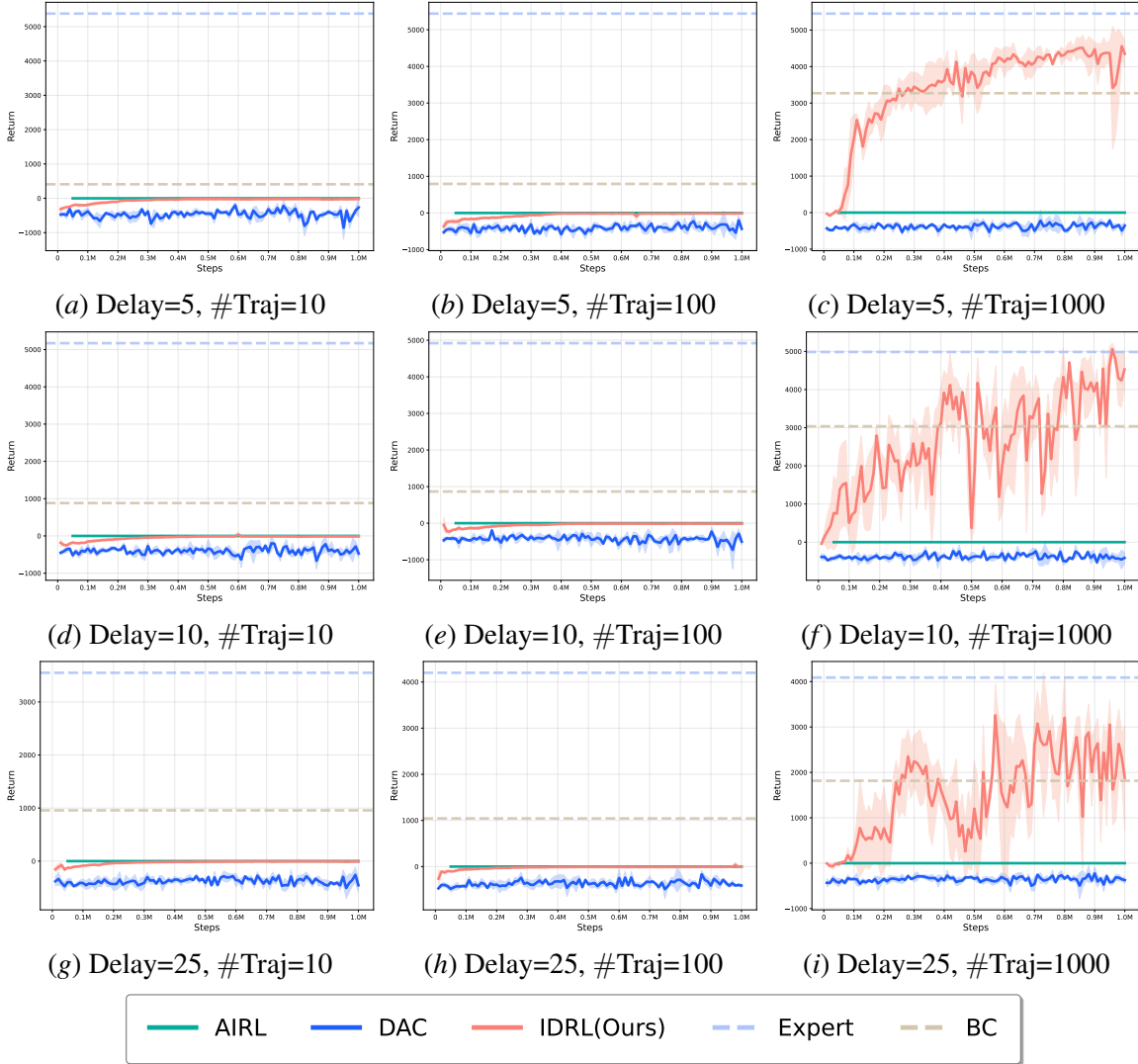


Figure 3: Learning Curves on HalfCheetah-v4 with different delays and quantities of expert demonstrations.

# INVERSE DELAYED RL

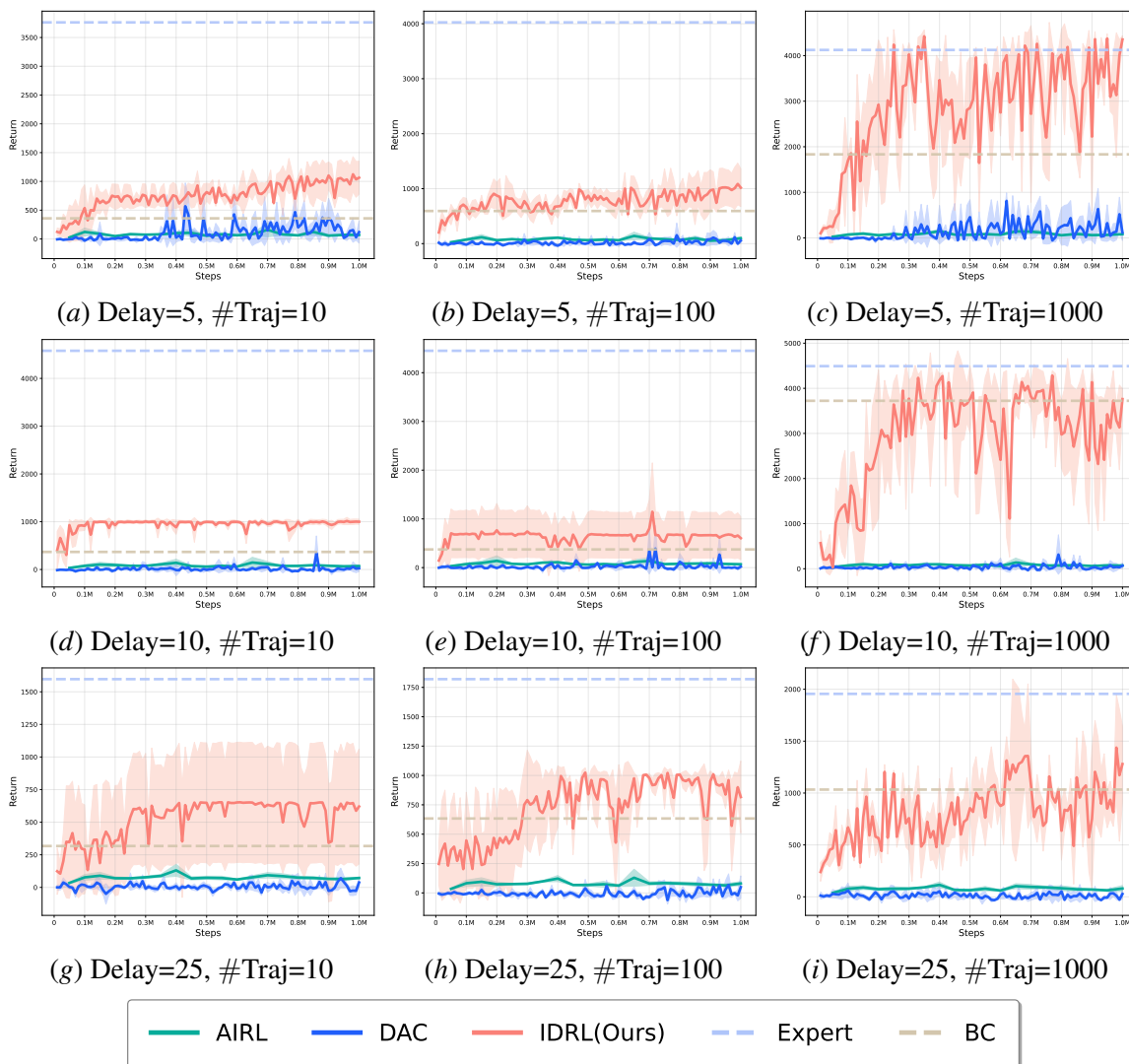


Figure 4: Learning Curves on Walker2d-v4 with different delays and quantities of expert demonstrations.

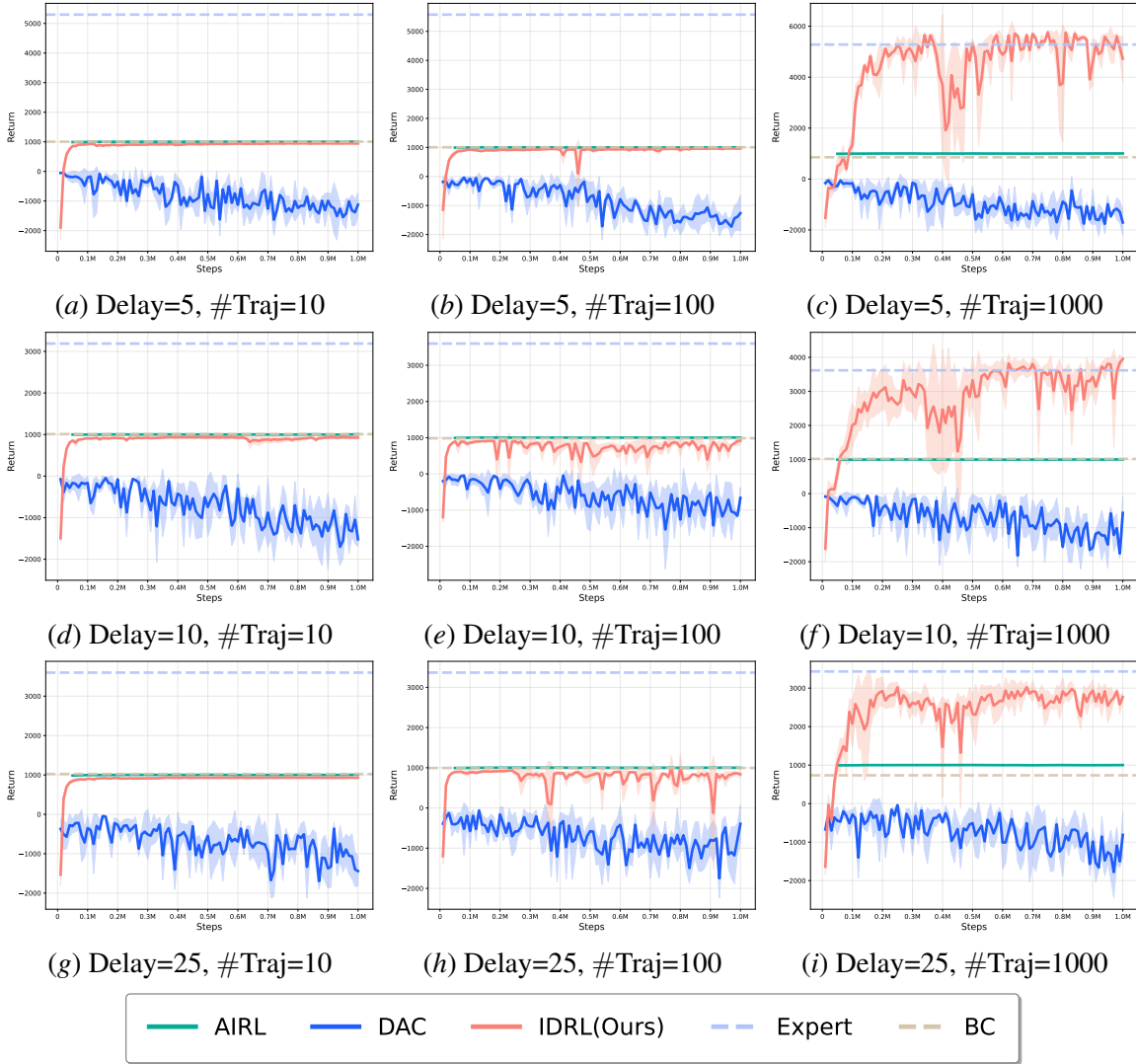


Figure 5: Learning Curves on Ant-v4 with different delays and quantities of expert demonstrations.



## Appendix C. Algorithm

---

**Algorithm 2** Auxiliary Delay Policy Optimization (Wu et al., 2024a)
 

---

- 1: **Input:** actor  $\pi_\psi$  for delay  $\Delta$ ; actor  $\pi_\phi^T$ , critics  $Q_{\theta_1}^T, Q_{\theta_2}^T$  and target critics  $\hat{Q}_{\theta_1}^T, \hat{Q}_{\theta_2}^T$  for auxiliary delays  $\Delta^T$ ; n-step  $n$ ; replay buffer  $\mathcal{D}$ ;
- 2: **for** each batch  $\{x_t, x_t^T, a_t, r_t : r_{t+n-1}, x_{t+n}, x_{t+n}^T\} \sim \mathcal{D}$  **do**
- 3:   Compute TD Target  $\mathbb{Y} = \sum_{i=0}^{n-1} [\gamma^i r_{t+i}] + \gamma^n \min(\mathbb{Y}_1, \mathbb{Y}_2)$ , where

$$\mathbb{Y}_1 = \mathbb{E}_{\hat{a} \sim \pi_\phi^T(\cdot | x_{t+n}^T)} [(Q_{\theta_1}^T(x_{t+n}^T, \hat{a}) - \log \pi_\phi^T(\hat{a} | x_{t+n}^T))],$$

$$\mathbb{Y}_2 = \mathbb{E}_{\hat{a} \sim \pi_\psi(\cdot | x_{t+n})} [(Q_{\theta_2}^T(x_{t+n}, \hat{a}) - \log \pi_\phi(\hat{a} | x_{t+1}))].$$

- 4:   Update  $Q_{\theta_i}^T (i = 1, 2)$  via applying gradient descent

$$\nabla_{\theta_i} [Q_{\theta_i}^T(x_t^T, a_t) - \mathbb{Y}].$$

- 5:   **if** Uniform(0, 1) > 0.5 **then**
- 6:     Update  $\pi_\phi^T$  via applying gradient descent

$$\nabla_\phi \mathbb{E}_{\hat{a} \sim \pi_\phi^T(\cdot | x_t^T)} \left[ \log \pi_\phi^T(\hat{a} | x_t^T) - \min_{i=1,2} Q_{\theta_i}^T(x_t^T, \hat{a}) \right].$$

- 7:   **else**
- 8:     Update  $\pi_\psi$  via applying gradient descent

$$\nabla_\psi \mathbb{E}_{\hat{a} \sim \pi_\psi(\cdot | x_t)} \left[ \log \pi_\psi(\hat{a} | x_t) - \min_{i=1,2} Q_{\theta_i}^T(x_t^T, \hat{a}) \right].$$

- 9:   **end if**
  - 10:   Soft update target critics weights  $Q_{\theta_1}^T, Q_{\theta_2}^T$  via copying from  $\hat{Q}_{\theta_1}^T, \hat{Q}_{\theta_2}^T$ , respectively.
  - 11: **end for**
  - 12: **Output:** actor  $\pi_\psi$ ;
-